Journal of Thermal Analysis and Calorimetry, Vol. 76 (2004) 165–177

SYNTHESIS AND THERMAL DECOMPOSITION OF LANTHANIDE HEXACYANOCHROMATE(III) COMPLEXES, $Ln[Cr(CN)_6]\cdot nH_2O$ (*Ln*=La–Lu; *n*=3, 4)

Y. Seto[1], *K. Umemoto*[1], *T. Arii*[2] *and Y. Masuda*[3*]

[1]Graduate School of Science and Technology, Niigata University, 2-8050 Ikarashi, Niigata 950-2181, Japan
[2]Thermal Analysis Division, Rigaku Corporation, 3-9-12 Matubara-cho Akishima, Tokyo 196-8666, Japan
[3]Department of Environmental Science, Faculty of Science, Niigata University, 2-8050 Ikarashi, Niigata 950-2181, Japan

(Received August 25, 2003; in revised form November 25, 2003)

Abstract

A series of lanthanide hexacyanochromate(III) *n*-hydrates, $Ln[Cr(CN)_6]\ nH_2O$ (*Ln*=La–Lu; *n*=3, 4) were synthesized as the precursors to obtain the homogeneous perovskite-type oxides, $LnCrO_3$. In the series of the hydrate complexes, $Nd[Cr(CN)_6]\ 4H_2O$ was the boundary between tetrahydrates and trihydrates, i.e. La, Ce, Pr and Nd formed tetrahydrates, and the other lanthanides formed trihydrates.

The crystal structures of $La[Cr(CN)_6]\ 4H_2O$ and $Sm[Cr(CN)_6]\ 3H_2O$ were determined by means of the Rietveld analysis of their powder X-ray diffraction profiles. $La[Cr(CN)_6]\ 4H_2O$ was orthorhombic system, *Cmcm*, and $Sm[Cr(CN)_6]\ 3H_2O$ was monoclinic system, $P2_1/m$.

The thermal decomposition of the series complex, $Ln[Cr(CN)_6]\ nH_2O$ was followed by means of thermal analyses, powder X-ray diffraction of the solid residue and the mass spectrum of the gaseous products. The homogeneous perovskite-type oxides, $LnCrO_3$ except of $CeCrO_3$ were obtained as the final products of the thermal decompositions. The perovskite oxides for La, Pr, Nd and Sm were formed at 800°C, for Eu, Gd, Tb and Dy at 1000°C, and for the other lanthanides at 1100°C. The final product of the thermal decomposition of $Ce[Cr(CN)_6]\ 4H_2O$ was the mixture of CeO_2 and Cr_2O_3.

Keywords: crystal structure, lanthanide hexacyanochromate(III) *n*-hydrates, perovskite-type oxides, thermal analysis, thermal decomposition

Introduction

Recently, perovskite-type oxides containing rare-earth ions and *d* transition metal ions such as $LaCrO_3$, $LaMnO_3$, $LaFeO_3$ and $LaCoO_3$ have been extremely interesting for their structure, electronic and magnetic properties [1–3]. The oxides, $LaMO_3$ (*M*=Cr, Mn, Fe and Co) have useful properties as high electrical conductivity, high

* Author for correspondence: E-mail: masuda@env.sc.niigata-u.ac.jp

1388–6150/2004/ $ 20.00

Akadémiai Kiadó, Budapest
Kluwer Academic Publishers, Dordrecht

melting point and anticorrosive. These mixed oxides also have been investigated for utilization in solid oxide fuel cell, refractory conducting materials, catalysts for the treatment of automobile exhaust and active materials for chemical sensor [4–8].

Generally, the solid state reaction method has been used to prepare the perovskite-type oxides because of its simple process. However, the method has some defects that it is very difficult to change the stoichiometric ratio of the metals of product, and the solid state reactions generally tend to produce less than optimum materials and require high calcining temperatures.

The other methods have been developed to prepare the high purity and homogeneous perovskite oxides, as sol-gel synthesis, hydrothermal reaction, coprecipitation techniques and thermal decomposition of heteronuclear complexes [9–14]. In 1968, one of the methods was proposed by Gallagher [15] to prepare $LaFeO_3$ and $LaCoO_3$ by use of the thermal decompositions of the appropriate hexacyano metallate complexes. Sadaoka [16] recently applied the method to prepare the oxides of $LnFeO_3$, $LnCoO_3$ and $Ln_xLn_{1-x}Fe_yCo_{1-y}O_3$ (*Ln*=La, Pr–Lu) by use of the thermal decompositions of $Ln[Fe(CN)_6]$ nH_2O, $Ln[Co(CN)_6]$ nH_2O and $Ln_xLn_{1-x}[Fe_yCo_{1-y}(CN)_6]$ nH_2O, respectively. This method is very useful to obtain homogeneous perovskite-type oxides at low temperatures.

$Ln[Fe(CN)_6]$ nH_2O and $Ln[Co(CN)_6]$ nH_2O were easily prepared by the reaction of $K_3[M(CN)_6]$ (*M*=Fe, Co) and LnX_3 (*Ln*=La–Lu; *X*=Cl, NO_3) in aqueous solution, and reported in detail their thermal and crystallographic properties [17–23]. However, it is difficult to obtain $Ln[Cr(CN)_6]$ nH_2O by means of the similar method because $K_3[Cr(CN)_6]$ is unstable and changes easily to $Cr(OH)_3$ in aqueous solution. Hulliger *et al*. prepared the complexes of $Ln[Cr(CN)_6]\cdot nH_2O$ in 1976 [24], but their structures and thermal properties have not yet been reported.

In this paper, the series of complexes, $Ln[Cr(CN)_6]$ nH_2O (*Ln*=La–Lu; *n*=3, 4) were synthesized in methanol solution, and the structures of $La[Cr(CN)_6]$ $4H_2O$ and $Sm[Cr(CN)_6]$ $3H_2O$ were determined by use of the Rietveld analysis of their powder X-ray diffraction profiles. The thermal decomposition process was also followed by means of thermal analyses (TG-DTA), powder X-ray diffraction (XRD) of the solid residue and the mass spectrum (TG-MS) of the gaseous products. The homogeneous perovskite-type oxides, $LnCrO_3$ except of $CeCrO_3$ were obtained as the final products of their thermal decompositions.

Experimental

Chemicals and preparations

Tetrabutylammonium hexacyanochromate(III), $(TBA)_3[Cr(CN)_6]$ was prepared as follows. When the aqueous solution of $K_3[Cr(CN)_6]$ was mixed with three times molar of tetrabutylammonium perchlorate methanol solution, potassium perchlorate, $KClO_4$ was deposited. After filtering out $KClO_4$, the filtrate was evaporated to dryness, the residue was dissolved in methanol and prepared the methanol solution of $(TBA)_3[Cr(CN)_6]$. The complexes of lanthanide hexacyanochromate(III) *n*-hydrates, $Ln[Cr(CN)_6]$ nH_2O

(*Ln*=La–Lu) were synthesized by adding equimolar of $Ln(NO_3)_3$ nH_2O to the methanol solution of $(TBA)_3[Cr(CN)_6]$.

Measurements

Thermogravimetry (TG) and differential thermal analysis (DTA) curves were simultaneously recorded on a Rigaku Thermoflex TAS200 TG-DTA in the temperature range from 20 to 1000°C at a heating rate of 10°C min^{-1}. About 10 mg of sample was weighed into a platinum crucible and the heating rate was 10°C min^{-1} in air [17–23].

The mass spectra (TG-MS) of the gaseous products evolved from the sample were monitored in dry helium and mixed atmosphere (O_2:He=1:4) with a Rigaku Thermo-Mass system, at the temperature ranges from 20 to 1200°C. In this system, the thermogravimetry and differential thermal analysis are simultaneously measured with the total ion current (TIC) of mass spectrometer, or the mass chromatogram on the basis of the selected *m/z* values to identify the evolved gases corresponding to the mass loss [19].

X-ray powder diffraction (XRD) profiles were obtained by means of a Rigaku Geigerflex RAD-3C diffractometer equipped with a high temperature sample holder. CuK radiation (=1.5418 Å) was monochromatized by use of a graphite monochrometer [25]. The X-ray generator was operated at the voltage of 40 kV and the current of 30 mA. The diffraction data were collected in the 2 range from 10 to 70° with a step-scan width of 0.02° and fixed time (5 s) counting procedure. The lattice parameters of $Ln[Cr(CN)_6]$ nH_2O (*Ln*=La and Sm) were determined by use of the CELL program [26], and the refinement of the structure was performed by means of the Rietveld method using the RIETAN2000 [27].

Results and discussion

The crystal structure of $Ln[Cr(CN)_6]\cdot nH_2O$

The XRD profile of $La[Cr(CN)_6]$ $4H_2O$ was similar to that of $La[Co(CN)_6]$ $5H_2O$. The crystal of $La[Co(CN)_6]$ $5H_2O$ is hexagonal and $P6_3/m$ [28]. Although the XRD profiles of both the complexes resemble to each other, the X-ray diffraction peaks of $La[Cr(CN)_6]$ $4H_2O$ shifted slightly into lower angles than those of $La[Co(CN)_6]$ $5H_2O$. Two crystal systems, i.e. hexagonal (a=7.683 and c=14.877 Å) and the orthorhombic (a=7.685, b=13.348 and c=14.877 Å), were predicted for $La[Cr(CN)_6]$ $4H_2O$ by use of the CELL program. The diffraction profiles were analyzed by means of the Rietveld refinement using these lattice parameters, and the degree of refinement was judged by the goodness of fit of S

$$S=R_{wp}/R_e$$

where R_{wp} is the weighed sum of residual of the least square fit and R_e is the value statistically expected.

The hexagonal ($P6_3$) and the orthorhombic ($Cmcm$ and $C222_1$) were attempted for the Rietveld refinement, and the space group of $Cmcm$ gave better refinement

than those of $P6_3$ and $C222_1$. Tables 1 and 2 showed the crystallographic data and fractional atomic coordinates. The observed profile can be thoroughly reproduced by use of these crystallographic parameters (Fig. 1). As compared with both the crystals of $La[Cr(CN)_6]\ 4H_2O$ and $La[Co(CN)_6]\ 5H_2O$, the eight-coordinated La atom has two coordinated water molecules in the former but the nine-coordinated La atom has three coordinated water molecules in the latter.

Table 1 Crystallographic data of $La[Cr(CN)_6]\ 4H_2O$

2 range/°	10–70
Step scan increment/°	0.02
Count time/s	5
Crystal system	orthorhombic
Space group	*Cmcm*
a/Å	7.7096 (6)
b/Å	13.3584(10)
c/Å	14.8248(4)
Reliability factors	
R_{wp}/%[a]	11.36
R_p/%[b]	8.35
R_c/%[c]	7.60
R_I/%[d]	3.34
R_F/%[e]	1.38
S[f]	1.49

[a] R – weighed pattern, [b] R pattern, [c] R – expected [d] R – integrated intensity, [e] R – structure factor
[f] S – the'Goodness-of-fit' indicator

Table 2 Fractional atomic coordinates of $La[Cr(CN)_6]\ 4H_2O$

Atom	Positions	x	y	z
La^{3+}	4c	0	0.3322(4)	1/4
Cr^{3+}	4a	0	0	0
C(1)	16h	0.318(3)	0.456(2)	0.0729(9)
C(2)	8f	0	0.145(3)	0.098(9)
N(1)	16h	0.211(2)	0.392(2)	0.098(3)
N(2)	8f	0	0.182(5)	0.120(1)
O(1)	8g	0.307(2)	0.246(1)	0.145(3)
O(2)	8f	0	0.6403(2)	0/4

Figure 2 shows the XRD profiles of the series complexes, $Ln[Cr(CN)_6]\ nH_2O$ (*Ln*=La–Lu). From the similarity of the XRD profiles, the crystal structures of $Ce[Cr(CN)_6]\ 4H_2O$, $Pr[Cr(CN)_6]\ 4H_2O$ and $Nd[Cr(CN)_6]\ 4H_2O$ are assumed to be orthorhombic and *Cmcm*.

The crystal structure of $Sm[Cr(CN)_6]\ 3H_2O$ was also presumed from the similarity of its XRD profile to that of $Sm[Co(CN)_6]\ 4H_2O$. The crystal of $Sm[Co(CN)_6]\ 4H_2O$ is orthorhombic and *Cmcm* [29]. The crystal system of $Sm[Cr(CN)_6]\ 3H_2O$ was expected to be monoclinic by use of the CELL program, and the lattice constants were a=7.542, b=14.025, c=7.482 Å and =119.70°. The Rietveld refinement was performed on the monoclinic and space group $P2_1/m$, and the reliability factor, the crystallographic data and the positional parameters are shown in Tables 3 and 4. The calculated profile was in

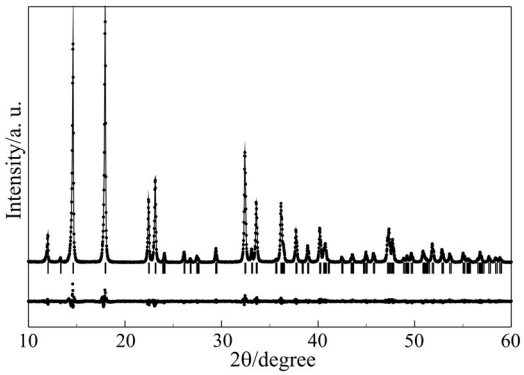

Fig. 1 Observed X-ray diffraction (dot) and calculated (line) profiles of $La[Cr(CN)_6]\ 4H_2O$ at room temperature. The bottom curve shows the difference of observed and calculated profiles, and the small bars indicate the angular positions of the allowed Brag refractions

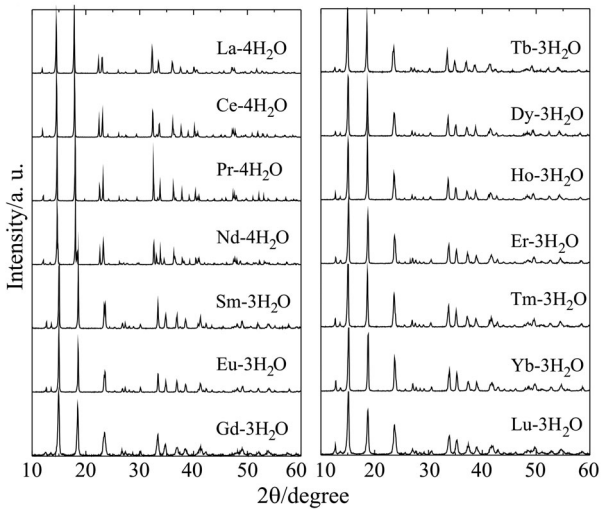

Fig. 2 XRD profiles of $Ln[Cr(CN)_6]\ nH_2O$ (*Ln*=La–Ln; n=3, 4)

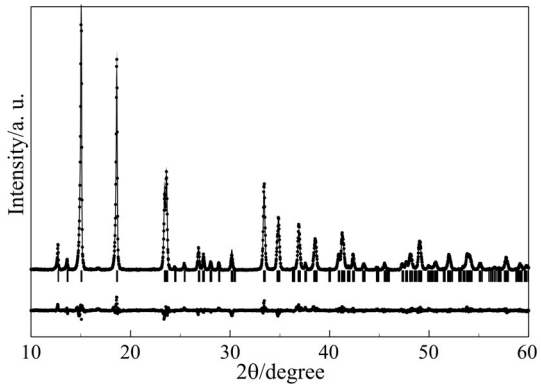

Fig. 3 Observed X-ray diffraction (dot) and calculated (line) profiles of $Sm[Cr(CN)_6]\ 3H_2O$ at room temperature. The bottom curve shows the difference of observed and calculated profiles, and the small bars indicate the angular positions of the allowed Brag refractions

fair agreement with the observed one as shown in Fig. 3. In the crystals of $Sm[Cr(CN)_6]\ 3H_2O$, one of the three water molecules coordinated to the Sm and the other two molecules were lattice water. The structures of the other hydrates, $Ln[Cr(CN)_6]\ 3H_2O$ (*Ln*=Eu–Lu) were estimated to be monoclinic and $P2_1/m$ from the similarity of their XRD profiles to that of $Sm[Cr(CN)_6]\ 3H_2O$ (Fig. 2).

Table 3 Crystallogrpahic data of $Sm[Cr(CN)_6]\ 3H_2O$

2 range/°	10–70
Step scan increment/°	0.02
Count time/s	5
Crystal system	monoclinic
Space group	$P2_1/m$
a/Å	7.5094(1)
b/Å	14.1177(6)
c/Å	7.575(1)
/°	119.98(1)
Reliability factors	
R_{wp}/%[a]	12.94
R_p/%[b]	9.35
R_c/%[c]	9.57
R_I/%[d]	3.54
R_F/%[e]	1.71
S[f]	1.35

[a] *R* – weighed pattern, [b] *R* pattern, [c] *R* – expected [d] *R* – integrated intensity, [e] *R* – structure factor
[f] *S* – the‘Goodness-of-fit’ indicator

Table 4 Fractional atomic coordinates of $Sm[Cr(CN)_6]\ 3H_2O$

Atom	Positions	*x*	*y*	*z*
La^{3+}	2e	0.3491(9)	1/4	0.6786(10)
Cr^{3+}	2a	0	0	0
C(1)	4f	0.075(6)	0.415(5)	0.846(6)
C(2)	4f	0.300(5)	0.555(2)	0.127(7)
C(3)	4f	0.150(9)	0.396(5)	0.293(7)
N(1)	4f	0.173(6)	0.362(3)	0.801(5)
N(2)	4f	0.451(3)	0.608(2)	0.248(5)
N(3)	4f	0.069(4)	0.334(2)	0.399(4)
O(1)	4f	0.670(4)	0.3912(8)	0.361(4)
O(2)	2e	0.543(6)	1/4	0.048(3)

Thermal dehydration and decomposition of $La[Cr(CN)_6]\cdot 4H_2O$

Figure 4 shows the TG-DTA curves for the thermal dehydration and decomposition of $La[Cr(CN)_6]\ 4H_2O$. Figure 5 showed the total ion current (TIC), which indicates sum of the ion current for all detectable species, and Fig. 6 illustrated the mass spectra of the gases detected at the TIC peaks. The mass spectra showed the evolution of H_2O at 127, 150 and 186°C. The complex was prepared in methanol solution, however, the thermal desolvation of methanol was not observed from the mass spectra. The dehydration took place through at least two stages. The mass loss (4.1%) for the first stage was accompanied by the endothermic peak at 88.1°C, and that for the second stage (12.7%) was by the two endothermic peaks at 151.9 and 154.2°C. The sum of these mass losses (16.8%) agreed approximately with the theoretical one for the four water molecules (17.1%) as follows

$$La[Cr(CN)_6]\ 4H_2O \quad La[Cr(CN)_6]\ 3H_2O + H_2O \text{ (first stage)} \quad (1)$$

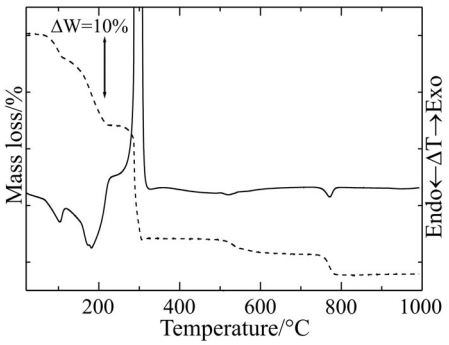

Fig. 4 TG-DTA curves for $La[Cr(CN)_6]\ 4H_2O$ (heating rate 10°C min^{-1} in air). – TG, – – DTA

$$La[Cr(CN)_6]\ 3H_2O \quad La[Cr(CN)_6]+3H_2O \text{ (second stage)} \quad (2)$$

These water molecules seemed to be arisen from the starting material, $La(NO_3)_3\ 6H_2O$.

After the dehydration, $La[Cr(CN)_6]$ decomposed subsequently and an abrupt mass loss was observed accompanying a vigorously exothermic peak at 276.9°C. The exthotherm would result from the oxidation of metals (La and Cr) and CN group, and the mass spectra measured at 320 and 325°C showed the evolution of CO_2 and N_2O, respectively, which is attributed to the cleavage of CN group.

A slow mass loss of 1.8% was found at the temperature range from 500 to 700°C, and another mass loss of 3.9% at around 770°C. Because any peak could not be recognized on the TIC for these mass losses, oxygen that is one of the components of mixed atmosphere, seemed to evolve at both the mass losses. In order to examine these mass losses, the XRD profiles were measured for the solid residues of $La[Cr(CN)_6]$ heated to several temperatures (Fig. 7). The phase obtained at 400°C was amorphous,

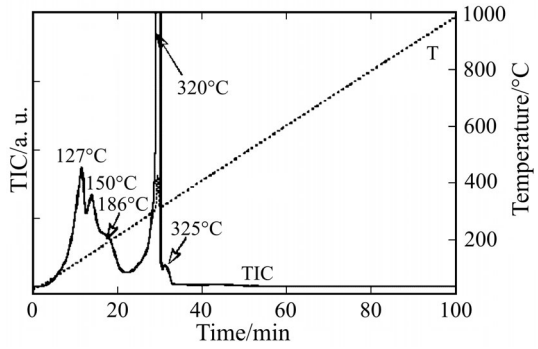

Fig. 5 Total ion currents (TIC) of $La[Cr(CN)_6]\ 4H_2O$

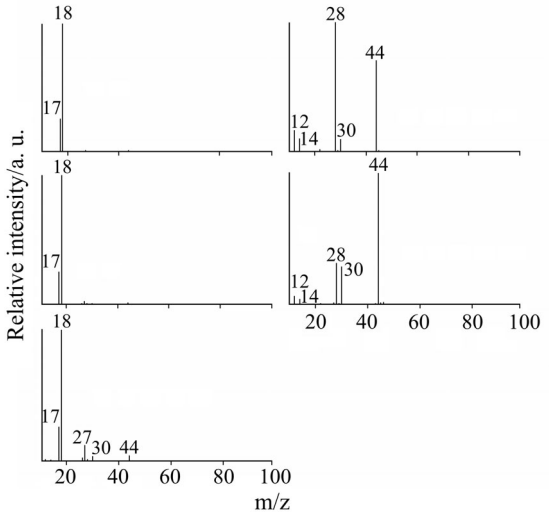

Fig. 6 Mass chromatograms obtained at 127, 150, 186, 320 and 325°C

but the phase obtained at 500°C was identified as $LaCrO_4$ [30]. The mass loss of 1.8% was accompanied with the complicating thermal behavior, i.e. endothermic and exothermic peaks were observed at 498 and 516°C, respectively (Fig. 8). The mass loss was compatible to the theoretical one (1.9%) for the endothermic reaction [31]

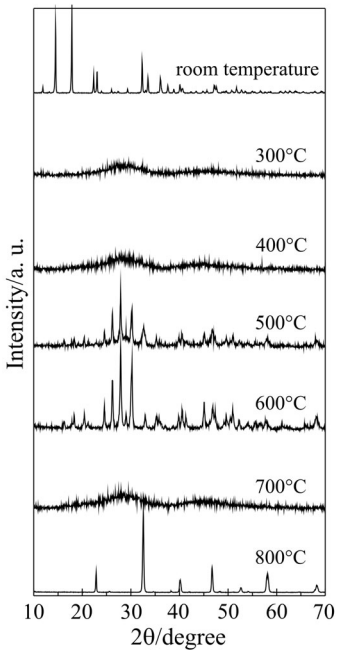

Fig. 7 XRD profiles of $La[Cr(CN)_6]$ $4H_2O$ heated to several temperatures

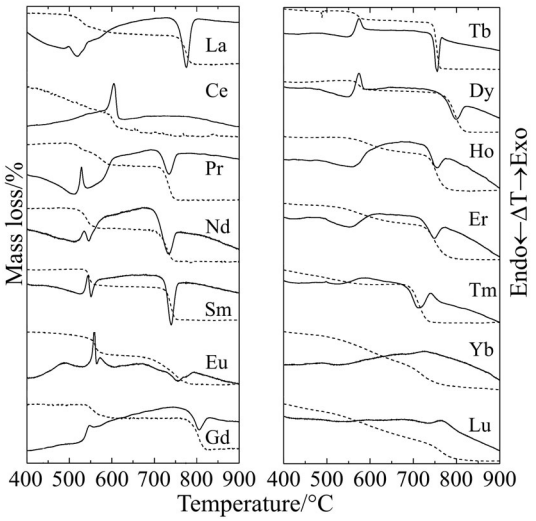

Fig. 8 TG-DTA curves of $Ln[Cr(CN)_6]$ nH_2O heating to the temperature ranges from 400 to 900°C

$$2La_2(CrO_4)_3 + La_2O_3 \quad 6LaCrO_4 + 1.5O_2 \tag{3}$$

The exotherm was attributable to the crystallization of the amorphous $LaCrO_4$ [12], which proceeded simultaneously with the endothermic reaction (3).

The phases obtained at 600 and 800°C were identified as $LaCrO_4$ and $LaCrO_3$, respectively [30, 32]. The mass loss of 3.9% accompanied with an endothermic peak at 779.6°C, was consisted with the value (3.8%) calculated for the reaction (4)

$$LaCrO_4 \quad LaCrO_3 + 0.5O_2 \tag{4}$$

The total mass loss expected for the reaction (5)

$$La[Cr(CN)_6]\ 4H_2O \quad LaCrO_3 \tag{5}$$

is 43.0%, which is in fair agreement with the observed one, 43.1%.

Thermal dehydration and decomposition of the other complexes

The TG-DTA curves of the series complexes, $Ln[Cr(CN)_6]\ nH_2O$ (*Ln*=La–Lu) were shown in Fig. 9. It was confirmed that $Nd[Cr(CN)_6]\ 4H_2O$ was the boundary between tetrahydrate and trihydrate, i.e. La, Ce, Pr and Nd formed tetrahydrates, and the other lanthanides formed trihydrates. This result was contrasted with that of the series hydrate complexes of $Ln[Co(CN)_6]\ nH_2O$ (*Ln*=La–Lu; *n*=4, 5). In the series complexes, $Ln[Co(CN)_6]\ nH_2O$, the lanthanide atoms lighter than Nd are known to form pentahydrates, hexagonal and $P6_3/m$, and the other complexes with heavier lanthanides than Nd are tetrahydrates, orthorhombic and *Cmcm*. The complex of Nd is known to form the pentahydrate, orthorhombic and $C222_1$, and $Nd[Co(CN)_6]\ 5H_2O$ has the boundary structure in the series complexes [17].

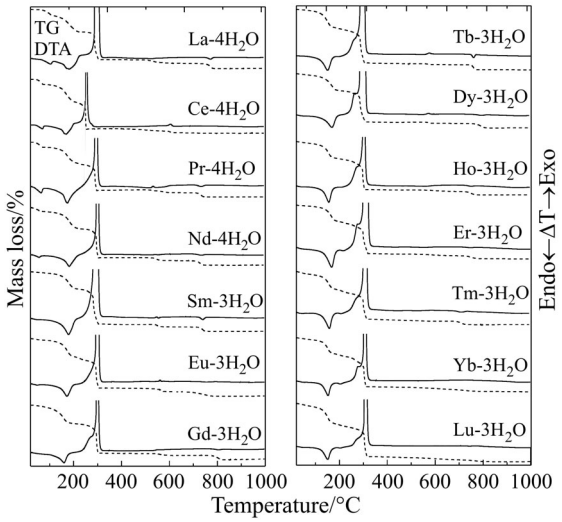

Fig. 9 TG-DTA curves of $Ln[Cr(CN)_6]\ nH_2O$ (*Ln*=La–Ln; *n*=3, 4; heating rate 10°C min^{-1} in air). – TG, – – DTA

The thermal dehydrations of $Ln[Cr(CN)_6]\ 4H_2O$ (*Ln*=Ce, Pr and Nd) were consisted of two stages as well as the case of La hydrate complex, but the two endothermic peaks for the second stage of $La[Cr(CN)_6]\ 4H_2O$ were overlapped in these hydrates. The first stage of the dehydration is corresponding to the loss of one coordinated water molecule, and the first endothermic peaks were recognized at 80.9, 58.6, 53.9 and 39.6°C for the hydrates of La, Ce, Pr and Nd, respectively. The decreasing the temperature of the first stage reflects the decreasing stabilities of these hydrates in this order. The result is explained by a combination of two factors which are correlated with the decrease of the ionic radii of the Ln^{3+} and contrary to each other, i.e. (1) increase of the effctive charge of Ln^{3+} with decreasing of the ionic radius of Ln^{3+}, enhances the interaction of Ln^{3+}–OH_2 bonds, and (2) decreasing of ionic radius leads to narrowing of the coordination sphere and then the mutual repulsion among the ligands contributes to the instability of Ln^{3+}–OH_2 bonds [20, 21]. The factor (2) seems to play more important role than that of (1) in the present hydrates, $Ln[Cr(CN)_6]\ 4H_2O$ (*Ln*=La–Nd). The thermal dehydration of the other hydrates took place in one stage corresponding to the second stage of La hydrate.

After the dehydration, $Ln[Cr(CN)_6]$ decomposed accompanying vigorous exotherms as the case of $La[Cr(CN)_6]$. Figure 10 shows the beginning temperature of the decomposition, which was estimated from the intersecting point of two tangential lines of TG curve. The temperatures for the series complexes except for Ce tend to increase slowly with increasing of atomic number. This finding indicates that the thermal stabilities of $Ln[Cr(CN)_6]$ may be increasing with decreasing of ionic radii of Ln^{3+} ions.

The oxides of $LnCrO_4$ and $LnCrO_3$ (*Ln*= Pr–Lu) were also formed at high temperatures according to the reactions (7) and (8) as the case of $La[Cr(CN)_6]$

$$2Ln_2(CrO_4)_3 + Ln_2O_3 \quad 6LnCrO_4 + 1.5O_2 \tag{7}$$

$$LnCrO_4 \quad LnCrO_3 + 0.5O_2 \tag{8}$$

The step of (7) for the complexes of Tm, Yb and Lu could not be observed clearly (Fig. 8). The homogeneous perovskite oxides, $LnCrO_3$ for La, Pr, Nd and Sm were formed at 800°C, for Eu, Gd, Tb and Dy at 1000°C and for Ho, Er, Tm, Yb and

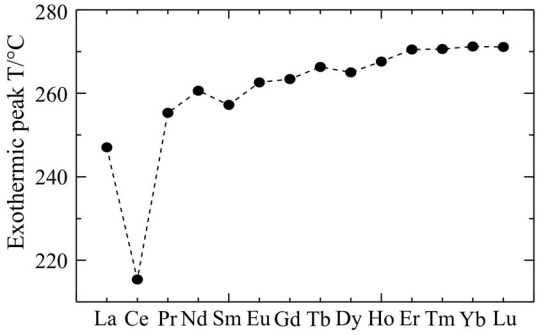

Fig. 10 The beginning temperatures of the thermal decompositions of the series complexes, $Ln[Cr(CN)_6]\times nH_2O$ (*Ln*=La–Ln; *n*=3, 4)

Lu at 1100°C (Fig. 11). It is interesting that the temperatures to obtain the single phase of perovskite oxides are increasing with atomic number of the lanthanide ion.

It is difficult to explain the thermal unstability of $Ce[Cr(CN)_6]\ 4H_2O$. A mass loss (3.8 %) took place at around 600°C and an exothermic peak was observed at 604°C (Fig. 8). The mass loss (3.8%) may be due to the reaction [33] (6)

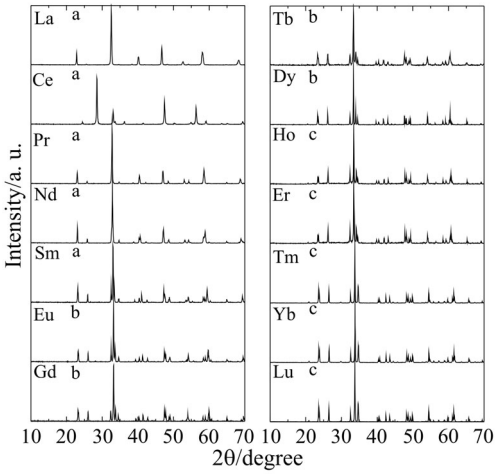

Fig. 11 XRD profiles of the final product of the thermal decomposition of $Ln[Cr(CN)_6]\ nH_2O$ (*Ln*=La–Ln; n=3, 4); a – obtained at 800°C, b – at 1000°C and c – at 1100°C

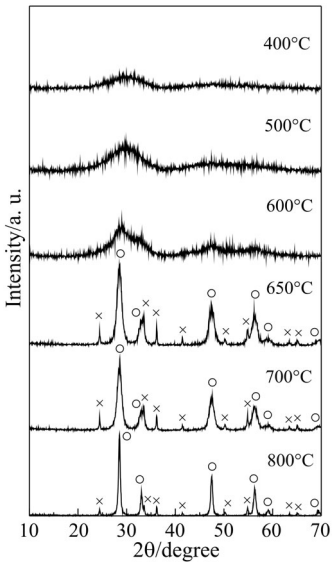

Fig. 12 XRD profiles of $Ce[Cr(CN)_6]\ 4H_2O$ heated to the temperature ranges from 400 to 800°C. ○ – CeO_2, × – Cr_2O_3

$$2CrO_2 \quad Cr_2O_3+0.5O_2 \qquad (6)$$

From the XRD profiles of the phase otained before and after the exothermic peak, the exothem was corresponded to the crystallization of amorpous phases of CeO_2 and Cr_2O_3 (Fig. 12). The perovskite oxide, $CeCrO_3$ could not be obtained from the thermal decomposition of Ce complex.

References

1 R. R. Heikes, R. C. Miller and R. Mazelsky, Physica, 30 (1964) 1600.
2 P. Sujatha Devi and M. Subba Rao, J. Solid State Chem., 98 (1992) 237.
3 P. Mahadevan, N. Shanthi and D. D. Sarama, J. Phys. Condens. Matter., 9 (1997) 3129.
4 V. Szabo, M. Bassir, J. E. Gallot, A. Van Neste and S. Kaliaguine, Applied Catalysis B: Environmental, 42 (2003) 265.
5 W. Z. Zhu and S. C. Deevi, Materials Science and Engineering A, 348 (2003) 227.
6 N. N. Toan, S. Saukko and V. Lantto, Physica B, 327 (2003) 279.
7 U. Casellato, P. Guerriero, S. Tamburini, S. Sitran and P. A. Vigato, J. Chem. Soc., Dalton Trans., 1991, 2145.
8 I. K. Murwani, S. Scheurell, M. Feist and E. Kemnitz, J. Therm. Anal. Cal., 69 (2002) 9.
9 T. Yao, Y. Uchimoto, T. Sugiyama and Y. Nagai, Solid State Ionics, 135 (2000) 359.
10 S. Bilger, G. Blab and R. Forthmann, J. Eur. Ceram. Soc., 17 (1997) 1027.
11 M. Yoshimura, S. T. Song and S. Somiya, J. Ceram. Soc. Jpn., 90 (1982) 91.
12 K. Azegami, M. Yoshinaka, K. Hirota and O. Yamaguchi, Mat. Res. Bull., 33 (1998) 341.
13 N. Deb, J. Therm. Anal. Cal., 67 (2002) 699.
14 O. Carp, L. Patron, A. Ianculescu, D. Crisan, N. Dragan and R. Olar, J. Therm. Anal. Cal., 72 (2003) 253.
15 P. K. Gallagher, Mat. Res. Bull., 3 (1968) 225.
16 Y. Sadaoka, New Development of Studies on Rare Earth Complexes 1997, p. 785.
17 Y. Yukawa, S. Igarashi, T. Kawaura and H. Miyamoto, Inorg. Chem., 35 (1996) 7399.
18 W. Xiaoyu, Y. Yukawa and Y. Masuda, J. Alloys Compds., 290 (1999) 85.
19 Y. Masuda, Y. Seto, X. Wang, Y. Yukawa and T. Arii, J. Therm. Anal. Cal., 60 (2000) 1033.
20 Y. Masuda, K. Minagawa, H. Ogawa, O. Nakazatao, Y. Yukawa and H. Miyamoto, J. Alloy. Comp., 235 (1996) 23.
21 Y. Masuda, K. Kikuchi, Y. Yukawa and H. Miyamoto, J. Alloy Comp., 250 (1997) 70.
22 Y. Masuda, Y. Seto, X. Wang and Y. Tuchiya, J. Therm. Anal. Cal., 64 (2001) 1045.
23 Y. Seto, S. Nagao, X. Wang and Y. Masuda, J. Therm. Anal. Cal., 73 (2003) 755.
24 F. Hulliger, M. Landolt and H. Vetsch, J. Solid State Chem., 18 (1976) 283.
25 Y.Masuda, A. Yahata and H. Ogawa, Inorg. Chem., 34 (1995) 3130.
26 Y. Takaki, T. Taniguchi and K. Hori, Seramikkusu Ronbunshi, 101 (1993) 373.
27 F. Izumi and T. Ikeda, Mater. Sci. Forum, 198 (2000) 321.
28 D. F. Mullica, W. O. Milligan and W. T. Kouba, J. Inorg. Nucl. Chem., 41 (1979) 967.
29 W. Petter, V. Gramlich and F. Hulliger, J. Solid State Chem., 82 (1989) 161.
30 Powder Diffraction File, Inorganic Volume, No.33-703 (1989).
31 A. Roy and K. Nag, J. Inorg. Nucl. Chem., 40 (1978) 1501.
32 Powder Diffraction File, Inorganic Volume, No. 24–1016 (1983).
33 M. Maciejewski, K. Kohler, H. Schneider and A. Baiker, J. Solid State Chem., 119 (1995) 13.